

Low Energy Measurements in Low-Energy μ SR

Andreas Suter¹, Maria Mendes Martins^{1,2}, Xiaojie Ni¹, Thomas Prokscha¹, Zaher Salman¹

¹ Paul Scherrer Institut, Laboratory for Muon-Spin Spectroscopy, CH-5232 Villigen PSI, Switzerland

² ETH Zürich, Advanced Power Semiconductor Laboratory, CH-8092 Zürich, Switzerland

E-mail: andreas.suter@psi.ch

Abstract. In the context of μ SR studies on magnetic materials in the ordered state, often a strong initial depolarization is found in the zero field spectra. For transverse field measurements this is often referred to as a loss in asymmetry. In case of the low-energy μ SR (LE- μ SR) setup this needs a more detailed discussion since effects such as time-of-flight distribution of impinging muons, back scattering, and muon reflection will change the spectra at early times and low implantation energies ($E < 3\text{keV}$). These effects are well understood and reproducible allowing to correct for in any given experiment. We will discuss them and show how to correct for in experiments at low implantation energies.

1. Introduction

Studies of magnetic systems with μ SR is of high interest since valuable information can be obtained, like the temperature dependence of the sub-lattice magnetization, magnetic fluctuation rates, the magnetic volume fraction, etc. Some of these classes of materials can change properties when grown as thin film. For instance tensile or compressive strain can be controlled by the choice of the substrate and can have strong effects on the magnetic properties. Some materials can only be grown as thin films. Sometimes these films can exclusively be stabilized at thicknesses $t < 20\text{ nm}$ which requires to work at rather low implantation energies $E < 3\text{ keV}$. Also, near surface properties on length scales of a few nanometer can be substantially different to the bulk. Especially for devices the bulk properties might not be all that relevant, but the concrete characteristics at interfaces or the near surface properties are crucial to be understood. Therefore it is essential to understand whether a naive straightforward interpretation of the data is applicable, or if there are additional instrumental effects present which need to be taken into account. As will be discussed in the following sections, there are indeed a couple of effects to be considered, typically not present in bulk- μ SR studies or LE- μ SR studies for $E > 3\text{ keV}$. All the presented low-energy μ SR data were measured at the muE4 beamline [1] at the Paul Scherrer Institut in Switzerland.

2. Backscattering

At low implantation energies there is some probability that a muon, after entering the sample, can be re-ejected from the bulk (backscattering). This is an effect typically not present in bulk- μ SR ($E \geq 4.1\text{ MeV}$). As discussed in Ref. [2], there is a high probability that such a backscattered muon is neutralized, *i.e.* forming muonium, when leaving the sample. This effect is almost



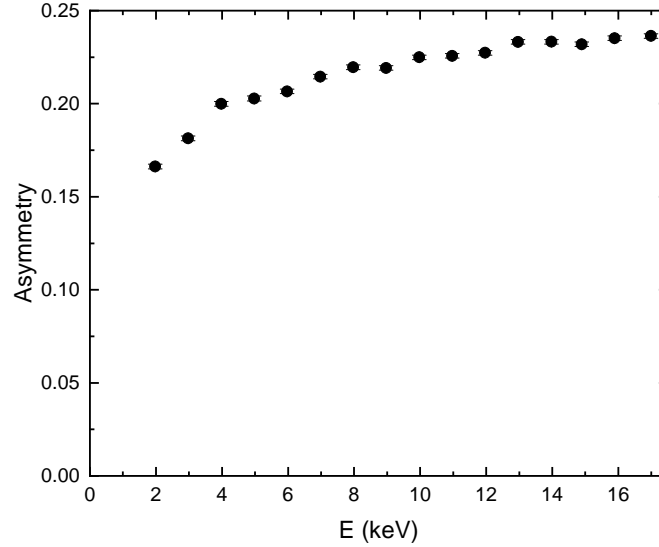


Figure 1. Asymmetry as a function of implantation energy measured in a transverse field of 10 mT.

independent on the properties of the target material. This has consequences when carrying out transverse field experiments. Since the muonium precession frequencies are significantly different to the muon Larmor frequency $\omega_{\mu^+} = \gamma_{\mu^+} B$, the asymmetry of the ω_{μ^+} signal will be reduced at low implantation energies. As discussed in detail in [2] the backscattering contribution can be estimated by the Monte Carlo code `trimsp` [3]. However, in large density materials, *e.g.* Au, there are some discrepancies. Fig. 1 shows the asymmetry versus the implantation energy for a standard Ag-coated sample plate of the LE- μ SR setup. The asymmetry is obtained from a transverse field experiment with $B = 10$ mT applied perpendicular to the initial muon spin at a temperature of $T = 200$ K. All μ SR data presented are analyzed with `musrfit` [4]. The figure shows that the transverse field asymmetry in LE- μ SR studies is depending on the implantation energy. If, for instance, the magnetic volume fraction of a material should be determined for a thin film (thickness $\lesssim 15$ nm), and the A_0 is not directly accessible since *e.g.* the magnetic transition temperature is experimentally not accessible, carefully calibration measurements for the given implantation energy and size of the sample is needed.

3. Time-of-Flight muon decay asymmetry distortions at early times

μ SR is an especially powerful method to study magnetic systems under zero field conditions. In the best case coherent zero field precession signals can be found which often allow to gain a deep insight in the underlying physics of the system. However, sometimes the zero field signal in the magnetic state takes the form

$$A(t) = A_0 [(1 - \alpha) \exp(-\lambda_F t) + \alpha \exp(-\lambda_S t)], \quad (1)$$

where A_0 is the full asymmetry at the given implantation energy, $\lambda_{F,S}$ is a fast, slow depolarization rate, and α is a weighting parameter. In case of a powder sample, $\alpha = 1/3$. There are various reasons why the low-temperature $A(t)$ takes the form as in Eq.(1), *e.g.* the internal field is so large, that the corresponding precession signal is higher than the instrumental

frequency resolution. Another reason could be that the magnetic field distribution is much broader than the central field and hence the system is overdamped. The latter might be caused by a complicated magnetic structure, or disorder. In magnetic systems, at low temperature, one often encounters $\lambda_F \gtrsim 10 \mu\text{s}^{-1}$.

Here enters a complication of the LE- μSR spectrometer, which we call time-of-flight (TOF) muon decay distortion, which occurs in the first 50–70 ns of the muon decay asymmetry spectra. The left side of Fig. 2 sketches the situation. For the time-differential μSR measurement a muon start signal is needed, followed by a “legal” positron stop signal. The muon start count detector is labelled on the sketch as trigger-detector (TD) or M-counter. The distance between the TD and the sample position is currently 563 mm. The speed of the μ^+ is $\simeq 4 - 5 \text{ mm/ns}$ (depending on the transport high voltage settings, *i.e.* the extraction energy of the slow μ^+ at the moderator). The red arrow sketches a μ^+ trajectory of a muon decaying (star) in the region of the last electrostatic focusing element (the ring anodes). The emitted positron (blue arrow) is registered by one of the positron detectors. Hence, this event will be considered by the DAQ as a “legal” event at early times of one of the positron decay histograms. Yet, of course, this has nothing to do with the studied sample. Since the ring anodes are made out of copper, the low energy positrons will be absorbed and hence not reaching the positron counters. This is leading to a seemingly increased asymmetry, since only the higher energy positrons are entering from the Michel spectrum (see Ref. [5]). The described effects are leading to seemingly fast decay of the asymmetry in the first 50 – 70 ns as shown on the right panels of Fig. 2. The top panel shows zero field measurement data for Ag at various temperatures and high voltage (HV) transport settings (Tr). The bottom panel is depicting transverse field data for Ag. As can be seen from the zero field data, as expected, there is no temperature dependence present. The speed of the μ^+ (HV transport settings) however, has a slight influence on the TOF muon decay asymmetry distortion. This is to be expected, since for the faster μ^+ (higher HV transport setting values) the distortion is less pronounced.

The TOF muon decay asymmetry distortion complicates the analysis of zero field measurements for which the asymmetry can be described by Eq. (1). Yet, still some valuable information can be obtained. Fig. 3 shows zero field spectra of a Ni coated sample plate at early times. Both signals are measured for the same transport settings and temperature. The difference is only the implantation energy of $E = 2 \text{ keV}$ and $E = 22 \text{ keV}$, respectively. The $E = 22 \text{ keV}$ spectrum shows the strongly damped zero field precession signal of Ni and a stronger λ_F depolarization. This means by combining different energies and/or temperature data, still valuable information can be obtained. For an example dealing with this complications see Ref. [6].

4. Muon Reflections

There is one more effect playing a role at low implantation energies which is muon reflection. In order to register incoming low-energy muons we use the so called trigger detector (see Ref. [7]). In essence the low-energy μ^+ is passing a thin carbon foil (thickness $\sim 2.2 \mu\text{g/cm}^2$, corresponding to ~ 50 atomic layers) and emits electrons which are detected by a micro channel plate detector (MCP). The total energy loss in the carbon foil varies for each μ^+ , resulting in an energy spread of the μ^+ beam after the carbon foil. Fig. 4 shows a typical energy spectrum for a transport setting of $\text{Tr} = 12 \text{ kV}$. Since the C-foil is on a potential of -3.48 kV , the kinetic energy of the μ^+ just before the C-foil is $E = 12 \text{ keV} + 3.48 \text{ keV} = 15.48 \text{ keV}$. The energy spectrum is obtained from a time-of-flight measurement of *muonium* from the TD to an MCP mounted at the sample position. Muonium forms in the carbon foil by charge-exchange collisions with a probability of about 10% at this energy [8]. The peak energy-loss is indicated by an arrow in Fig. 4. As one can see the energy spectrum is slightly asymmetric with a “tail” towards lower energies. In order to work at low implantation energies, the sample is positively biased, de-accelerating the μ^+ to the desired implantation energy. For instance for an implantation energy of $E = 1 \text{ keV}$ one can

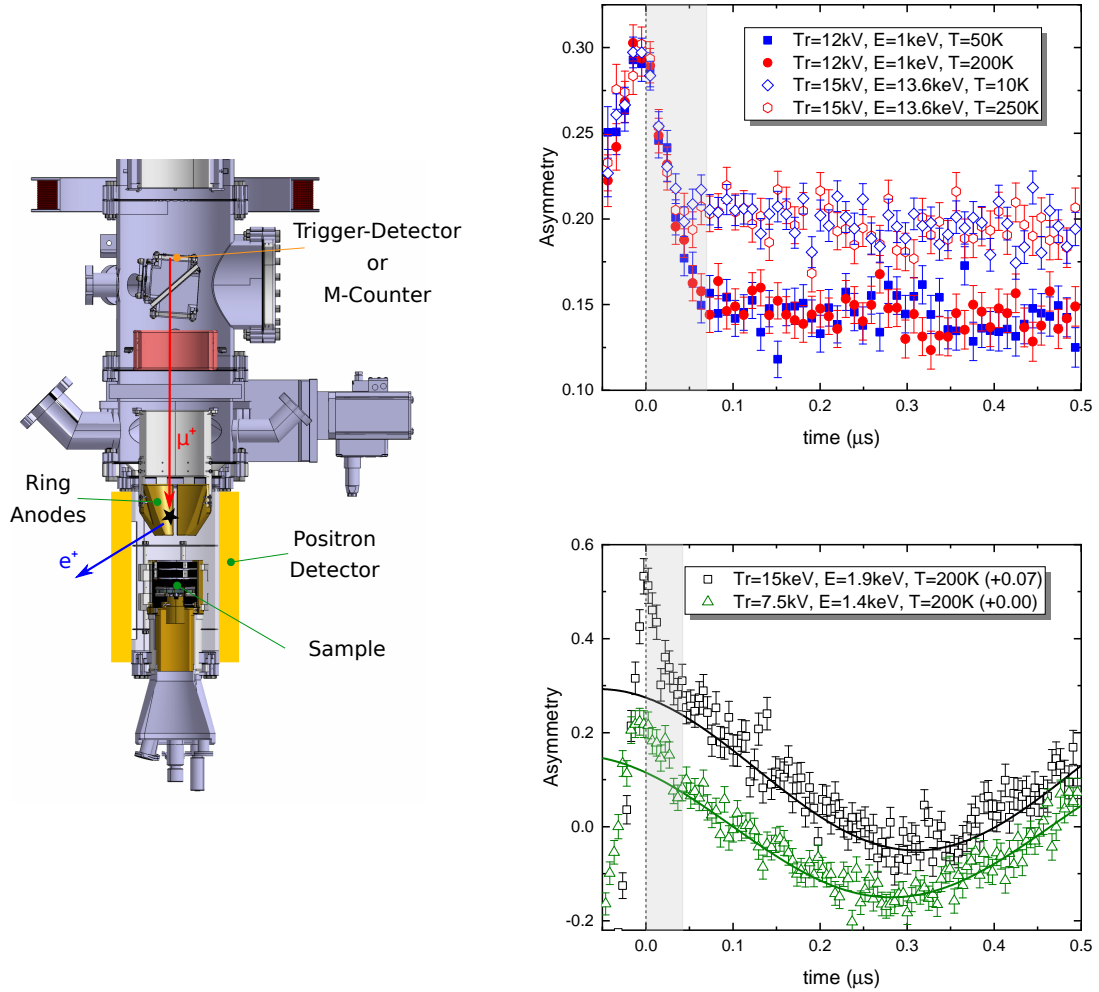


Figure 2. Left: Sketch of the early Time-Of-Flight (TOF) muon decay. Right Top: Ag zero field time spectra at early times. Right Bottom: Ag transverse field ($B = 10\text{mT}$) time spectra. For clarity the black signal is up-shifted by 0.07.

see from Fig. 4 that there is a low-energy tail of μ^+ having energies too low to be able to reach the sample (shaded area). This means, these μ^+ will not reach the sample but being reflected stopping most likely in the radiation shield which is in the current setup CuS coated. This effect is nicely visualized by the output of the musrSim/Geant4 simulation package [9]. Fig. 5 shows a couple of μ^+ trajectories (magenta). All the μ^+ shown correspond to ones from the shaded area in Fig. 4, *i.e.* they do not have sufficient energy to reach the positively biased sample.

To experimentally quantify the amount of reflected muons at very low implantation energies, we use a Ni coated sample plate. In a transverse field setup with $B = 10 \text{ mT}$ perpendicular to the muon spin and the sample plate, the asymmetry from muons stopping in the Ni layer is $A \lesssim 0.01$. On the other hand, muons being reflected will predominantly stop in the radiation shield of the cryostat. By fitting the precession signal this contribution can be quantified. The transverse field asymmetry of reflected muons, A_{refl} , versus its implantation energy is shown in Fig. 6. The energy dependence of A_{refl} can be well described by Eq. (2):

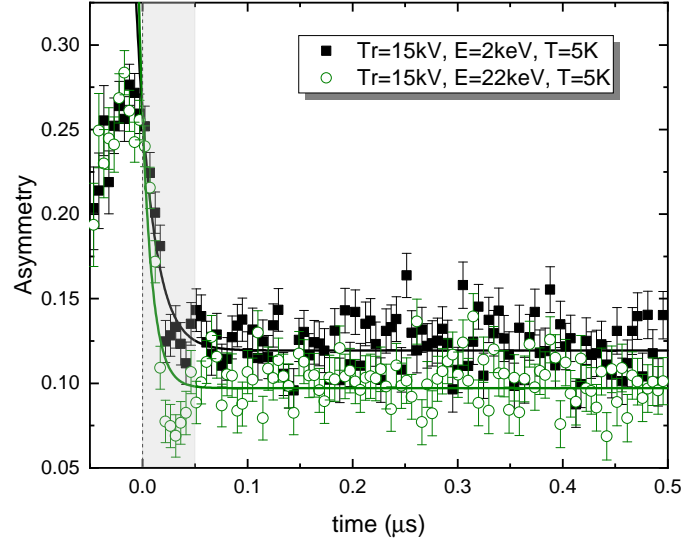


Figure 3. Ni coated sample plate. Zero field time spectra at $T = 5$ K for $E = 2$ keV and $E = 22$ keV.

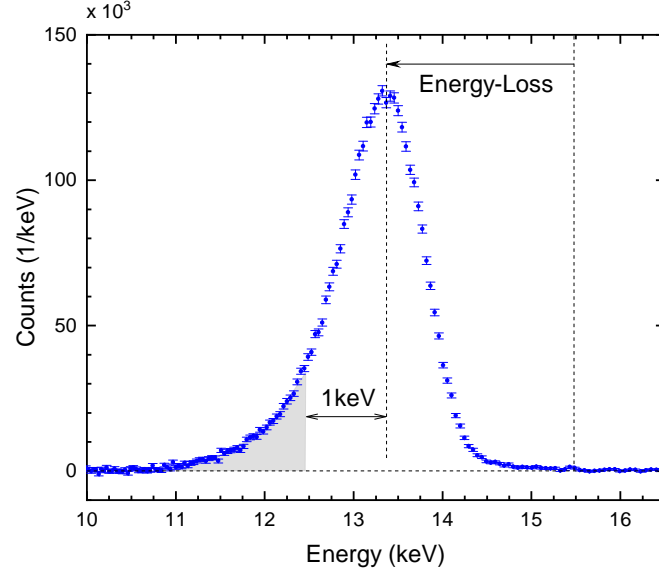


Figure 4. Background corrected energy-loss spectrum. Data from 2022, run 79, Transport settings 12kV. TD potential at the C-foil: -3.48 kV.

$$A_{\text{refl}}(E) = A_0 \exp(-E/E_0) + A_1. \quad (2)$$

E_0 is the energy scale over which reflection is relevant. A_0 is the amplitude, and A_1 is a “background” contribution which corresponds to the muons stopping in the Ni coated sample

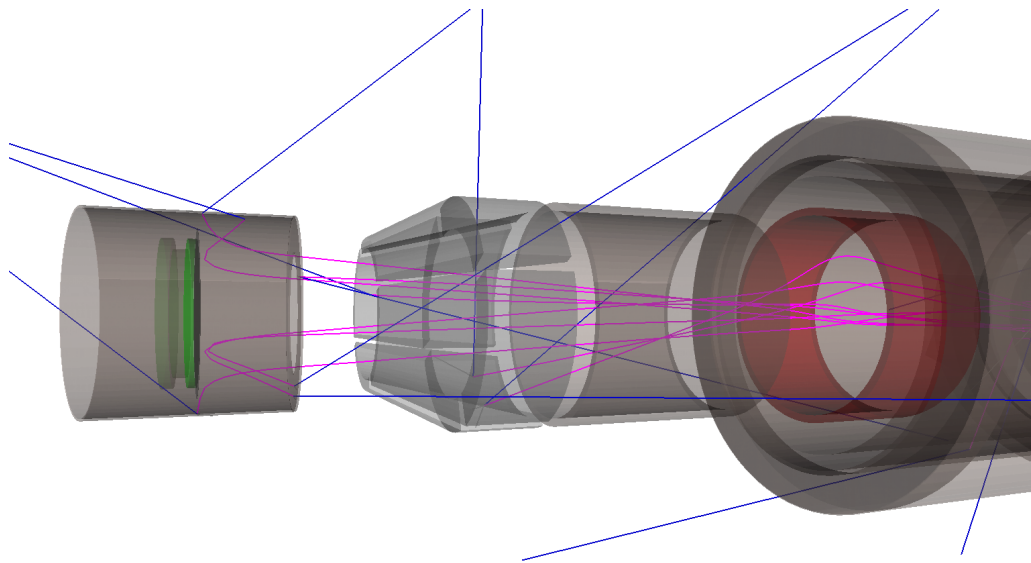


Figure 5. Muon reflection. The green plate is the sample. The magenta colored lines are muon trajectories. The blue lines represent decay positron trajectories. The grey cylinder around the sample plate is the radiation shield of the cryostat. Positron detectors, not shown, are cylindrically arranged around the sample plate, extending almost to the end position of the conically shaped ring anode segments in up-stream direction.

plate. This assignment and functional form has been verified by musrSim/Geant4 simulations. Fitting parameters for different transport settings are given in Table 1. To study the magnetic volume fraction of near surface regions ($E \lesssim 3$ keV), or very thin magnetic layers (thickness $t \lesssim 15$ nm) this contribution is relevant and needs to be corrected for. Eq. (2) together with the parameters of Table 1 allow to correct for this spurious contribution. For zero field measurements this is less straight forward.

Tr (kV)	A_0	E_0 (keV)	A_1
15.0	0.100(14)	1.83(22)	0.0095(10)
13.5	0.117(11)	1.42(15)	0.0106(12)
12.0	0.109(14)	1.19(16)	0.0107(13)

Table 1. Parameters according to Eq.(2) for different transport settings.

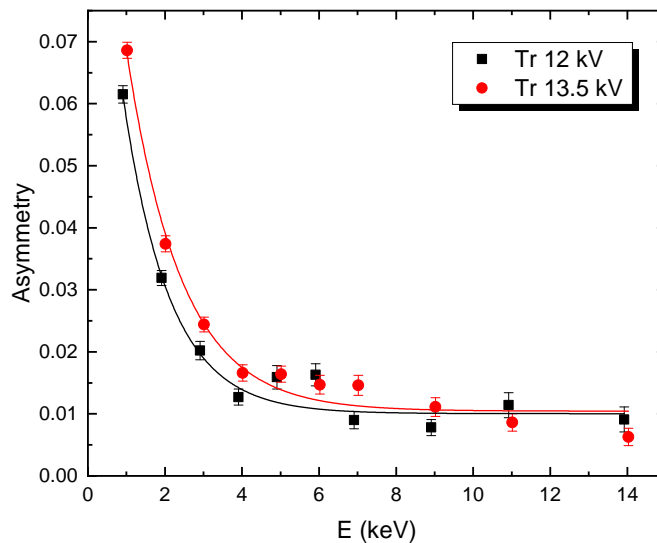


Figure 6. Transverse field asymmetry of reflected muons versus implantation energy for $B \leq 10$ mT. Lines are fits to the data according Eq. (2).

5. Conclusions

As discussed, there are various additional contributions present at very low implantation energies ($E < 3\text{keV}$) which need to be considered in the data analysis and interpretation of the LE- μSR data. These can be quantified by careful calibration experiments allowing to correct the data from these spurious contributions.

References

- [1] T. Prokscha, *et al.*, 2006 Physica B **374–375** 460.
- [2] E. Morenzoni, *et al.*, 2002 Nucl. Instr. and Meth. in Phys. Res. B **192** 254.
- [3] W. Eckstein, 1991 “Computer Simulation of Ion-Solid Interactions”, Springer, Berlin.
- [4] A. Suter and B.M. Wojek, 2012 Physics Procedia **30** 69.
- [5] F. Scheck, 1978 Physics Reports **44** 187.
- [6] J. Fowlie, *et al.* 2022 Nat. Phys. **18** 1043. <https://doi.org/10.1038/s41567-022-01684-y>.
- [7] E. Morenzoni, *et al.* 1997 Hyperfine Interactions **106** 229.
- [8] K.S. Khaw *et al.*, 2015 Journal of Instrumentation **10** P10025.
- [9] K. Sedlak, *et al.*, 2012 Physics Procedia **30** 61.